# Improved Retrieval of Cloud Liquid Water Path

*J. C. Liljegren*
*Ames Laboratory*
*Ames, Iowa*

## Introduction

The Atmospheric Radiation Measurement (ARM) Program has deployed dual-frequency microwave water radiometers (MWRs) (Liljegren 1994) at its Cloud and Radiation Testbed (CART) sites in the U. S. Southern Great Plains (SGP), the Tropical Western Pacific (TWP), and the North Slope of Alaska/Adjacent Arctic Ocean (NSA/AAO). Although the integrated water vapor amount provided by these instruments has enjoyed increasing application, the primary purpose of these instruments has been to provide measurements of the integrated liquid water path (LWP) in clouds.

Although the LWP measurements have been widely used by ARM investigators, shortcomings in the present statistical retrieval, with which the cloud LWP is derived from the microwave measurements, have become evident. Chief among these are the reliance on climatology in the estimation of the LWP. Not only does this require a separate retrieval (and an a priori data set) for each instrument location, but neither the synoptic and diurnal variations in the "dry" contribution to the microwave signal due to molecular oxygen nor the strong dependence of microwave emission by clouds on the temperature of the cloud water (and therefore on cloud height) are accounted for.

The objective of this research has been to develop a retrieval for cloud LWP that is 1) independent of local climatology and may thus be used at all ARM CART sites, 2) accounts for the variations in oxygen and liquid water contributions, and 3) is as simple as possible to accommodate real-time implementation in the microwave radiometer software.

## Background

The atmospheric opacity, $\tau$, at the measured microwave frequencies is due to the sum of a "dry" contribution, $\tau_{dry}$, from the far wing of the 60 GHz oxygen band, a contribution, $\tau_{vap}$, from the water vapor resonance centered at 22 GHz, and (for cloudy conditions) a contribution, $\tau_{liq}$, from liquid water

$$\tau = \tau_{dry} + \bar{\kappa}_{vap} V + \bar{\kappa}_{liq} L \tag{1}$$

where $\bar{\kappa}_{vap} = \tau_{vap} / V$ and $\bar{\kappa}_{liq} = \tau_{liq} / L$ are the (frequency-dependent) path-averaged mass absorption coefficients and $V = \int \rho_V dz$ and $L = \int \rho_L dz$ are, respectively, the precipitable water vapor and the integrated cloud liquid water. If the dry contribution is determined separately, it can be subtracted such that $\tau^* = \tau - \tau_{dry}$ and the two equations (one for each frequency) corresponding to (1) can be solved for the estimates of V and L

$$\begin{aligned} \hat{V} &= v_1 \tau_1^* + v_2 \tau_2^* \\ \hat{L} &= l_1 \tau_1^* + l_2 \tau_2^* \end{aligned} \tag{2}$$

where $v_1$, $v_2$, $l_1$, and $l_2$ are the "retrieval coefficients." The subscripts 1 and 2, respectively refer to the vapor- and liquid-sensitive frequencies (23.8 and 31.4 GHz). At each frequency, the opacity is calculated from the measured sky brightness temperature $T_{sky}$ as $\tau = \ln[(T_{mr}–T_c)/(T_{mr}–T_{sky})]$ where $T_c$ is the cosmic background radiating temperature (2.73 K) and $T_{mr}$ is the atmospheric mean radiating temperature.

## Retrieval Development

In order to apply this retrieval, the mean radiating temperature $T_{mr}$, oxygen contribution $t_{dry}$, and the retrieval coefficients $v_1$, $v_2$, $l_1$, and $l_2$ must be estimated. As shown in Table 1, extensive radiosonde data from ARM, Tropical Ocean Global Atmosphere-Coupled Ocean Atmosphere Response Experiment (TOGA-COARE) and the National Weather Service (NWS) were used to cover the full range of the parameter space for the retrieval.

Each sounding was integrated to determine V. For each profile, a microwave radiation transfer model (Schroeder and Westwater 1991) was used to calculate the three components of opacity $\tau_{dry}$, $\tau_{vap}$, and $\tau_{liq}$ as well as the mean radiating temperature, $T_{mr}$, and sky brightness temperature,

**Table 1**. Distribution of soundings. ⟨•⟩ indicates an ensemble mean; σ indicates the standard deviation.

| Site | Source | Number | $N_{clear}$ | $N_{cloudy}$ | $\langle P_{sfc}\rangle \pm \sigma_P$ (mb) | $\langle T_{sfc}\rangle \pm \sigma_T$ (K) | $\langle V\rangle \pm \sigma_V$ (cm) |
|---|---|---|---|---|---|---|---|
| Barrow, AK | NWS | 1720 | 711 | 1009 | 1016±11 | 261±13 | 0.71±0.57 |
| Manus Is., PNG | TOGA | 689 | 629 | 60 | 1010±2 | 301± 2 | 4.96±0.59 |
| Morris, OK | ARM | 1952 | 1358 | 594 | 990±6 | 294± 9 | 2.72±1.33 |
| Lamont, OK | ARM | 3369 | 2486 | 883 | 978±7 | 291±11 | 2.35±1.27 |
| Purcell, OK | ARM | 1319 | 947 | 372 | 975±6 | 292± 9 | 2.34±1.31 |
| Hillsboro, KS | ARM | 1812 | 1337 | 475 | 965±6 | 292±10 | 2.23±1.12 |
| Vici, OK | ARM | 1755 | 1339 | 416 | 943±6 | 293± 9 | 2.15±1.08 |
| Albuquerque, NM | NWS | 3063 | 2510 | 553 | 838±4 | 290±10 | 1.40±0.76 |
| PNG = Papua New Guinea | | | | | | | |

$T_{sky}$, at the two measurement frequencies. Because radiosondes do not measure liquid water, the model inserts clouds into the profile where the relative humidity exceeds 95%. In Table 1, soundings for which the relative humidity did not exceed 95% are classified as clear; the balance are classified as cloudy.

## Mean Radiating Temperature

For a given location, $T_{mr}$ correlates well with surface temperature and humidity. The surface pressure accounts for variations from location to location. For a wide range of locations and sky conditions $T_{mr}$ is estimated within ~2% from a linear regression on surface temperature, pressure and humidity.

## Oxygen Contribution

The "dry" contribution due to oxygen depends on the number of oxygen molecules overhead and thus is proportional to $(P\text{-}e)^2/T$, where P is the barometric pressure, e is the partial pressure due to water vapor and T is the absolute temperature, as shown in Figure 1. At all locations, the scatter increases with decreasing temperature due to meteorological conditions such as temperature inversions, for which the surface data are less representative of the vertical column.

The new retrieval uses measurements of surface pressure, temperature and humidity to directly account for the oxygen contribution. In this way the wandering (positive and negative) values of LWP for clear sky conditions that have often been misinterpreted as a lack of instrument sensitivity to thin clouds are addressed. Using this relationship, the oxygen contribution may be estimated for any location to within 2% to 3%.

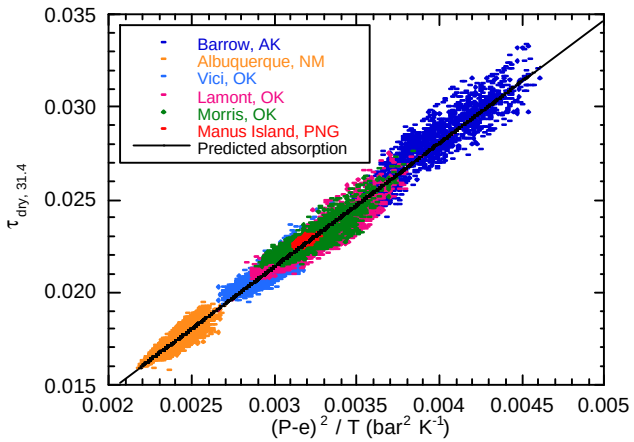


**Figure 1.** The "dry" contribution due to oxygen at 31.4 GHz for several locations as a function of pressure and temperature. The results at 23.8 GHz are very similar. (For a color version of this figure, please see *http://www.arm.gov/docs/documents/technical/conf_9803/liljegren-98.pdf*).

## Water Vapor Retrieval

The vapor coefficients, $v_1$ and $v_2$, exhibit a weak dependence on surface pressure; a weaker dependence on surface temperature and humidity is also evident. The coefficients of the vapor retrieval were fitted with a linear regression to the surface pressure, temperature and relative humidity. This permits $v_1$ and $v_2$, to be estimated within 2% for any location.

As a test, the new water vapor retrieval was applied the model-calculated brightness temperatures for the locations in Table 1. The results for each site are summarized in Table 2.

Only cloudy soundings were used to develop the new vapor retrieval (although both clear and cloudy soundings were used to develop the estimators for $T_{mr}$ and $t_{dry}$). The clear sky results therefore represent a semi-independent test of the algorithm. The new retrieval compares favorably with the statistical retrieval results. The bias in the statistical retrieval at Vici arises because Vici is over 600 m above sea level; whereas the statistical retrieval, based on soundings from Oklahoma City, was about 300 m above sea level. Note also the significant improvement in cloudy sky performance. The new retrieval was also applied to the MWR data from 1997 and compared against the statistical retrieval currently used at the SGP and other statistical retrievals derived specifically for the SGP central facility near Lamont, Oklahoma (see Figure 2).

The new location-independent retrieval compares well with the site-specific retrievals. The results in Figure 2 also demonstrate that the retrievals are independent of the radiosonde profiles used to derive them.

## Liquid Water Retrieval

Retrieval of the LWP is complicated by the fact that $\overline{\kappa}_{liq}$ decreases exponentially as liquid water temperature increases (see Figure 3), and thus depends strongly on the height and thickness of the cloud. Consequently, the liquid water retrieval coefficients, $l_1$ and $l_2$, also exhibit a strong dependence on cloud water temperature. Although the mean cloud liquid temperature is difficult to measure

**Table 2**. Means and standard deviations of the differences between the precipitable water vapor (in millimeters) estimated both by the new retrieval and the statistical retrieval currently in use at the SGP sites, and that calculated from the soundings for each site, for clear and cloudy conditions.

| | Clear | | | | Cloudy | | | |
|---|---|---|---|---|---|---|---|---|
| **Retrieval** | **New** | | **Current** | | **New** | | **Current** | |
| **Site** | $\langle\Delta V\rangle$ | $\sigma_V$ | $\langle\Delta V\rangle$ | $\sigma_V$ | $\langle\Delta V\rangle$ | $\sigma_V$ | $\langle\Delta V\rangle$ | $\sigma_V$ |
| Barrow, AK | -0.07 | 0.31 | | | -0.11 | 0.22 | | |
| Manus Island, PNG* | -0.03 | 0.31 | | | 0.13 | 0.40 | | |
| Morris, OK | -0.14 | 0.40 | -0.19 | 0.35 | -0.10 | 0.52 | -0.34 | 0.47 |
| Hillsboro, KS | -0.01 | 0.34 | 0.17 | 0.29 | -0.01 | 0.40 | -0.00 | 0.40 |
| Lamont, OK | 0.05 | 0.35 | 0.08 | 0.32 | 0.04 | 0.43 | -0.15 | 0.43 |
| Purcell, OK | -0.04 | 0.37 | 0.08 | 0.31 | -0.09 | 0.51 | -0.16 | 0.43 |
| Vici, OK | 0.04 | 0.32 | 0.43 | 0.35 | -0.04 | 0.44 | 0.25 | 0.41 |
| Albuquerque, NM | 0.04 | 0.14 | | | -0.16 | 0.27 | | |
| PNG = Papua New Guinea | | | | | | | | |

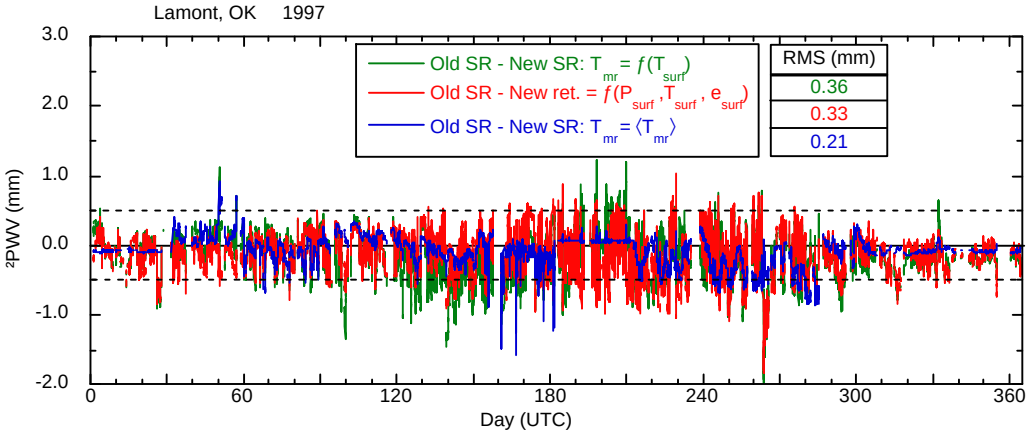


**Figure 2.** Differences (in precipitable millimeters) between the current statistical retrieval (derived from NWS soundings at Oklahoma City) and the new retrieval are shown in red for 1997. For comparison, differences with statistical retrievals (derived from ARM soundings launched at the SGP central facility) using monthly-averaged values of $T_{mr}$ (blue) and $T_{mr}$ estimated from surface data (green) are also shown. 30-minute averages are shown; periods of precipitation have been removed. (For a color version of this figure, please see *http://www.arm.gov/docs/documents/technical/conf_9803/liljegren-98.pdf*).

directly, it may be approximated by the cloud base temperature and measured with a narrowband infrared sensor at 10 µm. (ARM uses EG&G Hiemann model KT19.85 pyrometers with a band pass of 9.6 µm to 11.5 µm for this purpose.) This approximation works well for single-layer clouds that are sufficiently thin that their average temperature is close to their base temperature.

The approach taken here is to determine the liquid water retrieval coefficients for thin clouds having a mean temperature close to the base temperature in order to correctly describe the relationship between the retrieval coefficients and the cloud water temperature, and then to develop a correction to the base temperature to account for finite cloud thickness.

If the cloud is sufficiently thick that its average temperature is significantly less than its base temperature, then the LWP will be over-predicted. The situation is worse if multiple cloud layers are present where significant liquid water exists in the upper layer(s). To accommodate the effect of finite cloud thickness and reduce the effect of multiple cloud layers, a corrected cloud liquid temperature is calculated by assuming an adiabatic liquid water distribution and pseudo-adiabatic temperature distribution within the cloud. From these, the liquid-weighted average cloud temperature is computed.

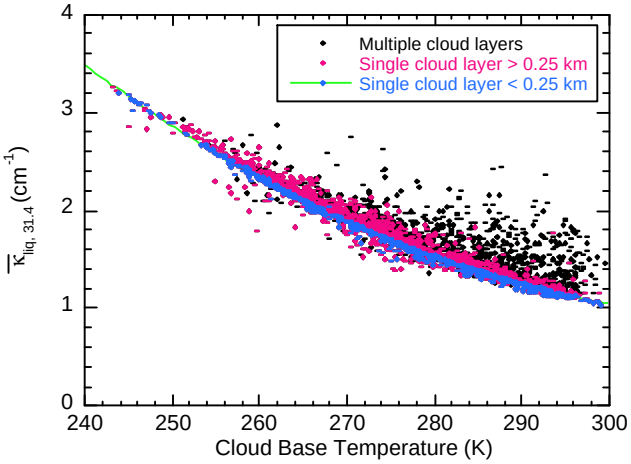


**Figure 3**. The path-averaged liquid water absorption coefficient at 31.4 GHz for single and multiple cloud layers correlated with cloud base temperature. The behavior at 23.8 GHz is similar. (For a color version of this figure, please see *http://www.arm.gov/docs/documents/technical/conf_9803/liljegren-98.pdf*).

For large precipitable water vapor amounts, the infrared temperature at 10 µm will be warmer than the actual cloud base temperature due to a contribution from water vapor emission. A correction has been developed for this as well.

The advantage of accounting for cloud temperature is revealed in Figure 4 wherein the difference in LWPs for the new and current retrieval is plotted as a function of the corrected cloud liquid water temperature.

Figure 4 reveals that the current retrieval overestimates the LWP of cold clouds and underestimates warm clouds relative to the new retrieval, which accounts for cloud water temperature. This is due to the climatological average liquid water temperature implicit in the current statistical retrieval.

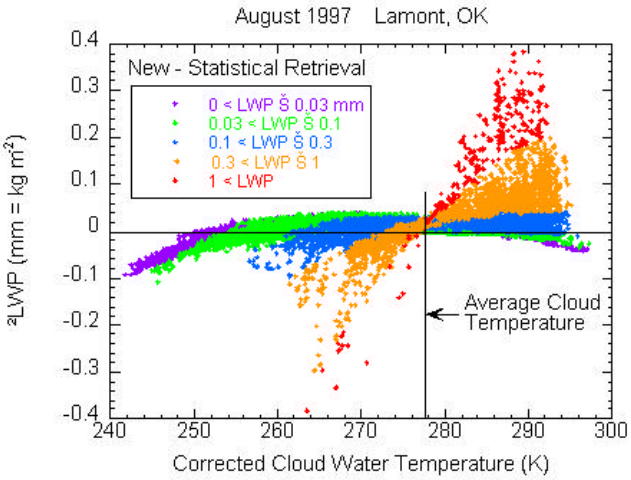


**Figure 4.** Liquid water path difference (new retrieval minus current statistical retrieval) as a function of the corrected cloud water temperature during August 1997 at the ARM site near Lamont, Oklahoma. (For a color version of this figure, please see *http://www.arm.gov/docs/documents/technical/conf_9803/liljegren-98.pdf*).

# References

Liljegren, J. C., 1994: Two-channel microwave radiometer for observations of total column precipitable water vapor and cloud liquid water path. Preprints of the *Fifth Symposium on Global Change Studies*, January 23-28, 1994, Nashville, Tennessee.

Schroeder, J. A., and E. R. Westwater, 1991: User's guide to WPL microwave radiative transfer software. NOAA Tech. Memo. ERL WPL-213.